Systematic screen for human disease genes in yeast

Lars M. Steinmetz[1,3*], Curt Scharfe[2,3*], Adam M. Deutschbauer[1], Dejana Mokranjac[4], Zelek S. Herman[3], Ted Jones[3], Angela M. Chu[2], Guri Giaever[3], Holger Prokisch[4], Peter J. Oefner[2,3] & Ronald W. Davis[1–3]

*These authors contributed equally to this work.

Published online: 22 July 2002, doi:10.1038/ng929

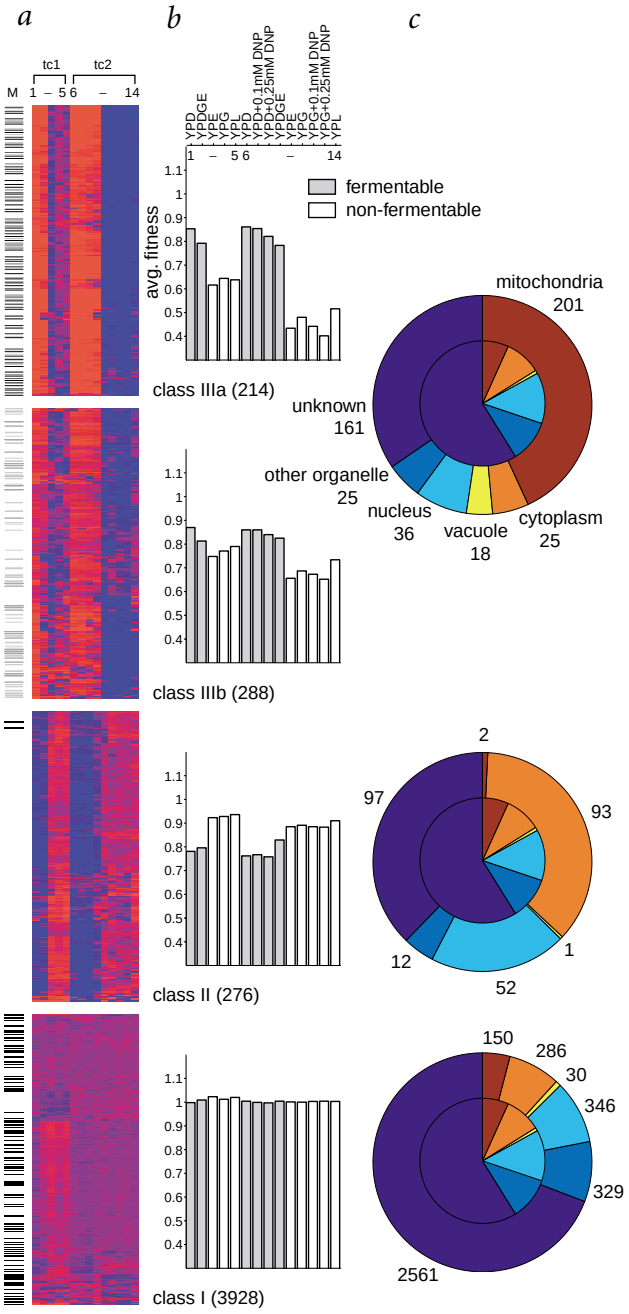

Fig. 1 Categorization of the whole genome according to phenotypes associated with gene deletions. ***a***, Clustergram showing four fitness patterns found among the 4,706 homozygous diploid deletion strains in the pool. Each row represents a strain with a deletion of a different gene and each column a different medium condition. The number of strains in each cluster is indicated in parentheses next to the cluster name. For each strain, fitness values are indicated with a color scale ranging from blue to red, with blue representing levels below, and red levels above, the strain's median. Conditions 1–5 represent measurements from the first experimental time course (tc1) and columns 6–14 those from a repeat experiment (tc2). Marked in black at left are 353 strains with deletions of genes previously known to localize to or function in mitochondria (M). ***b***, The bar graphs show the average fitness profiles for each cluster. For each condition, the height of the bar represents the growth rate of strains in the cluster relative to the average growth rate of the pool. Values of 1.0 indicate no difference, those less than 1.0 strains that grow more slowly than, and those greater than 1.0 strains that grow more quickly than, the pool average. The medium conditions, indicated above the graphs, are in the same order as the columns in the clustergram. ***c***, The outer pie chart shows the composition of genes represented in each cluster according to MIPS localization categories[22], after the removal of all spurious ORFs. The inner pie charts represent the distribution over the genome. Because of the similarity in pattern, the class III clusters were combined.

High similarity between yeast and human mitochondria allows functional genomic study of *Saccharomyces cerevisiae* to be used to identify human genes involved in disease[1]. So far, 102 heritable disorders have been attributed to defects in a quarter of the known nuclear-encoded mitochondrial proteins in humans[2]. Many mitochondrial diseases remain unexplained, however, in part because only 40–60% of the presumed 700–1,000 proteins involved in mitochondrial function and biogenesis have been identified[3]. Here we apply a systematic functional screen using the pre-existing whole-genome pool of yeast deletion mutants[4–6] to identify mitochondrial proteins. Three million measurements of strain fitness identified 466 genes whose deletions impaired mitochondrial respiration, of which 265 were new. Our approach gave higher selection than other systematic approaches, including fivefold greater selection than gene expression analysis. To apply these advantages to human disorders involving mitochondria, human orthologs were identified and linked to heritable diseases using genomic map positions.

The yeast deletion collection is a quantitative tool for systematically measuring the contribution to survival and reproduction (fitness) of most genes in the yeast genome[7]. In this study, 5,791 heterozygous diploid and 4,706 homozygous diploid deletion strains were quantitatively measured and monitored in parallel in 9 different medium conditions. Adapting classic diagnostic tests of mitochondrial function, we measured the growth (fitness) of mutant strains on non-fermentable substrates (including glycerol, lactate and ethanol) and compared

[1]*Department of Genetics and* [2]*Department of Biochemistry, Stanford University School of Medicine, Stanford, California 94305, USA.* [3]*Stanford Genome Technology Center, Palo Alto, California 94304, USA.* [4]*Insitute of Physiological Chemistry, University of Munich, Munich, Germany. Correspondence should be addressed to C.S. (e-mail: curts@stanford.edu) and L.M.S. (e-mail: larsms@stanford.edu).*

it with growth on fermentable sugar (glucose). Mutants with respiratory defects have impaired growth on non-fermentable substrates and are classically defined as 'petite'[8,9].

Of the 425 previously known genes encoding proteins involved in mitochondrial function and biogenesis[10], we detected the deletion strains for 353 in the homozygous diploid deletion pool (Fig. 1*a*). Of the remainder, the deletions were either lethal (37) or not successfully made (9), or the strains yielded signals too low to be considered detectable in the pool (26). Fifty-seven percent (201 of 353) of the mutants showed defects in growth on non-fermentable substrates, suggesting that about half of all mitochondrial-related proteins are essential for optimal respiratory activity[11] and can therefore be identified by a quantitative growth selection screen. The defects affected functions including oxidative phosphorylation, the tricarboxylic acid (TCA) cycle, mitochondrial protein synthesis and transport, ionic homeostasis and the metabolism of vitamins, cofactors and prosthetic groups. Mitochondrial genes whose deletion did not result in growth defects (152) encoded proteins with functions redundant or secondary to respiration: outer membrane transport, nucleotide transport and amino-acid metabolism.

In the heterozygous diploid pool, we observed few growth deficiencies, suggesting that mitochondrial proteins and enzymes were expressed in excess of minimum levels. In a small number of cases, including four strains heterozygous for deletions of known mitochondrial proteins (Rim2, Atp16, Nam9 and Mrpl19), we observed defects in growth on non-fermentable substrates, and the corresponding homozygous deletion mutant was lethal or not detected.

To identify new mutants with deficiencies in growth on non-fermentable substrates, we clustered the 4,706 quantitative homozygous diploid fitness profiles into four classes. Class I comprised 3,928 mutants (83.5%) with equal fitness on all the nutrients tested; class II comprised 276 with a higher fitness on non-fermentable substrates; and classes IIIa and IIIb comprised 502 with more and less severe defects, respectively, in fitness on non-fermentable substrates (Fig. 1*a*,*b*). We focused on class III for further analysis.

As physically overlapping genes cannot be distinguished by deletion analysis, we eliminated overlapping open reading frames (ORFs) that were defined as spurious[12], thereby reducing the number of genes in class III to 466. Because in these cases we detected the same phenotype for both overlapping ORFs, the spurious ORFs served as internal controls and validated our screen. Of the 466 genes, 201 (43%) encoded proteins with known mitochondrial localization or function[10]; 104 (22%), proteins that localized outside the mitochondria with functions in vacuolar and ion transport, transcription, and protein targeting, sorting and translocation; and 161 (35%), proteins with unknown subcellular localization, and in most cases unknown function (Fig. 1*c*).

We suspected that about half of the 161 proteins designated as unknown were localized to the mitochondria. Fifty-one had a putative mitochondrial import sequence[13], and 20 were homologous to sequences in *Rickettsia prowazekii*, which may be the closest ancestor of mitochondria[14] and has a total of 110 homologs of class III genes. Five of the 161 physically interacted with a known mitochondrial protein[15], and 21 had been identified as mitochondrially localized in a recent high-throughput immunolocalization study[16]. For six unknown proteins that each had a putative mitochondrial import sequence and were encoded by a gene whose deletion produced a severe phenotype, we assessed mitochondrial import directly using radiolabeled precursor proteins and isolated yeast mitochondria. Five of the six (Rsm18, Ygr101w, Yil157c, Mhr1 and Ppt2) were post-translationally imported into the mitochondria in a membrane potential–dependent manner. For Rsm18, Ygr101w and Yil157c, import was accompanied by removal of the signal peptide (Fig. 2).

Most mitochondrial proteins are encoded by the nuclear genome and are dependent on cellular protein expression and transport. The additional finding of nuclear (36) and cytoplasmic proteins (25) with defects in growth on non-fermentable substrates was therefore expected[2,17] (Fig. 1*c*). These genes integrate mitochondria into the cellular network, and their discovery illustrates an advantage of functionally based screening. Finding 68 cytoplasmic ribosomal proteins and 52 nuclear proteins whose absence led to deficient growth on fermentable substrates (class II) confirmed that the demand for translation[18] and transcription[19] is higher during fermentation than during respiration. In addition, combinations of defects in growth on fermentable and non-fermentable substrates were observed for genes of the glycolytic metabolic pathway (Fig. 3).

Two lines of evidence further confirmed the specificity of the quantitative deletion screen. First, for most proteins of the TCA cycle and respiratory chain, the corresponding deletion strains had defects in growth on non-fermentable substrates (Fig. 3). Second, genes encoding known mitochondrial proteins were 6.1-fold more enriched in our candidate set (class III) than in the genome (Fig. 1*c*). In comparison, gene-expression analysis of the diauxic shift[19] revealed an enrichment factor of only 1.2. As the diauxic shift represents a change in carbon source from glucose to ethanol and hence a shift from fermentation to respiration, the conditions are comparable to those of our growth selection screen. The enrichment data suggested that deletion phenotype is a more specific measure of gene function than is expression level. Twenty-four percent of genes whose deletion resulted in a

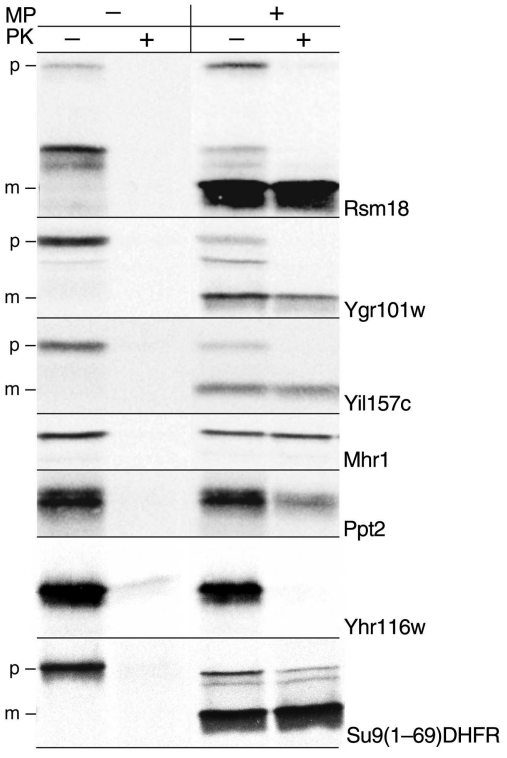

Fig. 2 Verification of mitochondrial candidates by import. Samples were derived by incubating radiolabeled proteins with mitochondria in the presence or absence of a membrane potential (MP) and the presence or absence of proteinase K (PK). In cases where import was accompanied by removal of the signal peptide, the precursor protein is labeled p; m indicates mature protein; Su9(1–69)DHFR, positive control.

defect in growth on non-fermentable substrates displayed at least a twofold difference in expression; conversely, 7% of genes with changing expression showed such a growth defect.

Rather than being used to infer the function of a gene from its expression level, expression analysis can also provide a detailed molecular phenotype, or signature profile. This approach produced a better agreement with our quantitative deletion screen. When we considered expression as a phenotype, 14 of 24 deletions of known mitochondrial proteins were clustered into the same group because they had a statistically similar signature profile[20]; in turn, our approach identified the same 14, as well as a further 3. The drawback of signature profiling, however, is that it requires one experiment per deletion strain and thus thousands of arrays to measure all strains, compared to only a single array at each time point for the deletion screen.

When we extended our screen to humans, we found 255 human orthologs of class III yeast genes associated with defects in growth on non-fermentable substrates (see Web Table A online). Of these, 21 were genes known to be involved in mitochondrial disease inherited in a mendelian fashion. These included genes encoding two subunits of complex II of the respiratory chain, five assembly factors of complex III and IV and six proteins associated with deficiencies of mitochondrial multienzyme complexes (Fig. 4). Additionally, eight orthologs were found associated with diseases for which a mitochondrial pathophysiology is plausible but has not been proved. In turn, for 33 of 102 known human genes associated with mendelian mitochondrial disease, there was no corresponding yeast gene whose deletion was associated with growth defects, although in a few cases (including *ALD4*, *GUT2* and *YBR208C*) the deletion strains showed minor deficiencies. A further 15 of the 102 were not measured in our screen (and hence were either lethal or not detectable) and 33 yielded no yeast orthologs (see Web Table B online). Although our systematic screen for human disease genes in yeast was therefore by no means comprehensive, these data showed that many human disease genes are associated with a wide spectrum of yeast deletion phenotypes and can be identified through quantitative growth selection in yeast.

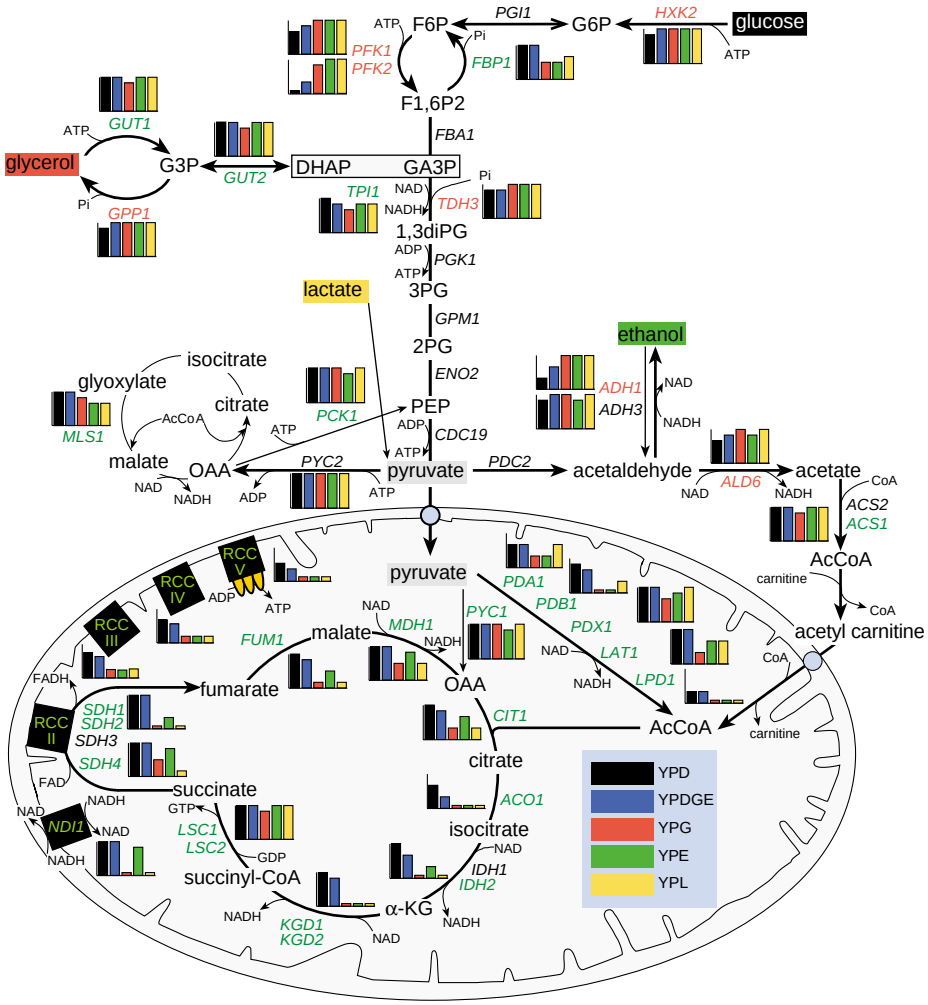

Fig. 3 Distinction between mitochondrial and cytoplasmic pathway branches: glycolysis above and TCA cycle and mitochondrial respiratory chain below. The bar graphs indicate the relative fitness of a homozygous deletion mutant of a gene under different medium conditions, color-coded in the legend. Genes without bar graphs were not detected. For the respiratory-chain complexes (RCC) III, IV and V, an average profile is shown. Deletions of genes shown in red lettering result in deficiency in growth on fermentable substrates, and deletion of those in green in a deficiency in growth on non-fermentable substrates. Ac, acetyl; CoA, coenzyme A; DHAP, dihydroxyacetone phosphate; 1,3diPG, 1,3-bisphosphoglycerate; F6P, fructose-6-phosphate; F1,6P2, fructose-1,6-bisphosphate; GA3P, glyceraldehyde-3-phosphate; α-KG, α-ketoglutarate; OAA, oxaloacetate; PEP, phosphoenolpyruvate; 2PG, 2-phosphoglycerate; 3PG, 3-phosphoglycerate; Pi, phosphate.

To propose specific new disease candidates, we selected seven mapped, putative mitochondrial disorders for which affected individuals have either symptoms characteristic of recorded mitochondrial diseases or biochemical findings indicative of mitochondrial pathophysiology. We analyzed a candidate set of 406 previously known human mitochondrial proteins[10] as well as 259 new proteins identified in our study that were either orthologs to class III proteins or new orthologs to previously known yeast mitochondrial proteins (see Web Table A online). We assigned 24 as candidate genes to reported disease intervals (Table 1). These included 11 new disease candidates identified directly by their class III quantitative deletion phenotype in yeast.

The 6.1-fold enrichment of mitochondrial proteins in the yeast deletion screen exceeded the selection achieved by other systematic, functional, genome-wide approaches. The integration of these data with localization, interaction and other functional information will advance studies of mitochondria in a cellular context. For human diseases, the new genes promise to accelerate positional cloning by serving as candidates for mutational screens in mendelian and complex mitochondrial disorders. Similar approaches may be applicable to other categories of human disease.

Fig. 4 Human mitochondrial-related genes that give rise to disease and for which there is an associated quantitative deletion phenotype in yeast. Bar graphs represent the relative fitness of homozygous yeast deletion mutants grown in different carbon sources, as defined in the legend of Fig. 3. AA, amino acid; DH, dehydrogenase; KG, ketoglutarate; QDP, quantitative deletion phenotype; RCC, respiratory-chain complex.

QDP	Yeast gene	Human gene	OMIM	Pathophysiological defect
	*SDH1*	*SDHA*	600857	RCC II subunit
	*SDH2*	*SDHB*	185470	RCC II subunit
	*BCS1*	*BCS1L*	603647	RCC III assembly
	*SHY1*	*SURF1*	185620	RCC IV assembly
	*SCO1*	*SCO1*	603644	RCC IV assembly
	*SCO1*	*SCO2*	604272	RCC IV assembly
	*COX10*	*COX10*	602125	RCC IV assembly
	*LAT1*	*PDX1*	245349	pyruvate DH
	*PDA1*	*PDHA1*	312170	pyruvate DH
	*PDA1*	*BCKDHA*	248600	AA catabolism (DH)
	*PDB1*	*BCKDHB*	248611	AA catabolism (DH)
	KGD2	*DBT*	248610	AA catabolism (DH)
	*LPD1*	*DLD*	246900	pyruvate/AA/α-KGDH
	*MIS1*	*MTHFD1*	172460	AA metabolism
	GCV3	*GCSH*	238330	AA metabolism
	*YHM1*	*SLC25A15*	603861	small-molecule transport
	PET8	*SLC25A15*	603861	small-molecule transport
	*FUM1*	*FH*	136850	TCA-cycle enzyme
	MIP1	*POLG*	174763	maintenance of mtDNA
	*HEM14*	*PPOX*	600923	heme biosynthesis
	YTA12	*SPG7*	602783	ATP-dependent protease
	*CCC2*	*ATP7B*	277900	copper-transport ATPase

Methods

Deletion screen and array hybridization. We made pools from strains of the yeast deletion project by transferring approximately equal amounts of individual deletion strains from frozen stocks onto YPD plates containing G418 (300 μg/ml). After 3 d of growth, cells were scraped off the plates and pooled. We grew an overnight culture of the deletion pool in YPD (1% Bacto-peptone (Difco), 2% yeast extract and 2% glucose). In addition, we cultured in a separate pool 422 homozygous diploids and 660 heterozygous diploids that showed low abundance after overnight growth. On initiation of the time course, we mixed the main and supplementary pools and placed aliquots in separate flasks containing 100 ml YPD (2% glucose), YPDGE (0.1% glucose, 3% glycerol and 2% ethanol), YPE (2% ethanol), YPG (3% glycerol), YPL (2% lactate), or (two flasks each) YPD or YPG containing 0.1 mM and 0.25 mM dinitrophenol, an uncoupling agent. We grew aerobic batch cultures in the presence of 50 μg/μl carbenicillin, to minimize the chance of bacterial contamination, for five generations to an A_{600} of 0.5 or less and then rediluted the cultures into fresh medium before repeating the process. We sampled the cultures every five generations for a total of 20 generations and repeated the measurements in YPD, YPDGE, YPE, YPG and YPL in a second experiment.

We isolated genomic DNA from each collected sample using standard rapid glass-bead lysis. Because there were two DNA tags engineered into each deletion strain, PCR reactions were carried out on the genomic DNA separately for the upstream and downstream tags (primer sequences are available on request). We used 2.5 μg of nucleic acid template (without RNase treatment) in a 30-cycle PCR reaction. Equal aliquots of upstream and downstream PCR reactions were mixed and hybridized to Affymetrix DNA_Tags_3 arrays as previously described[4].

Statistical calculations. CEL data files generated by Affymetrix GeneChip software contained the intensity values of each probe on the array. We normalized arrays of different generations from the same culture by adjusting the mean value of all perfect-match probes to a common value. Because each strain is marked with two different tags on average, four intensity measurements (for sense and antisense probes for each tag) are obtained per strain per time point, and therefore provide redundancy that serves as an internal control. As 5 time points were collected, there were in most cases 20 data points per strain per medium. Only intensity measurements three times the background level were considered meaningful. Time courses for each medium that derived from the same starter culture were analyzed in a batch. Regression lines were fitted to the logarithm of the intensity for the first three time points, applying two criteria: (i) regression lines for different media but for the same probe on the array had to pass through the same starting point, marking the time when the starter culture was split equally into the different media; and (ii) regression lines calculated for different probes for a given

Table 1 • Candidate genes associated with putative human mitochondrial-related diseases

Putative mitochondrial-related disorder	OMIM	Cytogenic location	Genetic markers flanking disease interval	Interval location (cM)	New human candidates in interval; marked (*) if yeast deletion phenotype	Previously known human candidates in interval; marked (*) if yeast deletion phenotype
Spastic paraplegia 5A	270800	8p12–q13	*PLAT–D8S279* (ref. 23)	64.6–91.5	*CGI-11*[a] (*) *LOC85479*[a] (*) *PDE7A* (*)	*MRPL15* (*)
Friedreich ataxia, FRDA2	601992	9p23–p11	*D9S285–D9S1874* (ref. 24)	27.9–59.9	*ACO1* (*) *DNAJA1* (*) *MGC14836*[a] *SR-BP1*[a] (*)	*NDUFB6* *ALDH1B1*
Optic atrophy, OPA4	605293	18q12.2–q12.3	*D18S34–D18S479* (ref. 25)	62.3–71.3	*DKFZP667C165*[a] (*)	*ATP5A1*(*) *ACAA2*
Optic atrophy, OPA2	311050	Xp11.4–p11.21	*DXS993–DXS991* (ref. 26)	66.1–86.9	*APEXL2*[a] (*) *PFKFB1* (*)	*TIMM17B* *ALAS2*
Neuropathy, motor-sensory type II, with deafness	310490	Xq24–q26	*DXS425–HPRT* (ref. 27)	126.3–152.5	*PLS3* (*)	*NDUFA1* *SLC25A14* *PDCD8*
Ptosis, hereditary congenital 2	300245	Xq24–q27.1	*DXS1047–DXS984* (ref. 28)	150.3–159.5	*MGC14797*[a] (*)	*SLC25A14* *PDCD8*
Mental retardation with optic atrophy, deafness	309555	Xq26	*DXS424–DXS297* (ref. 29)	116.8–167.3	*PLS3* (*) *MGC14797*[a] (*)	*SLC25A5* *NDUFA1* *SLC25A14* *PDCD8* *SLC9A6* (*)

[a]UniGene identifier for putative genes not listed in HUGO nomenclature database.

strain in the same medium had to be parallel and could therefore be represented by a single regression slope. For easier reading, we added 1.0 to the regression slopes, yielding a value of 1.0 for a lack of change in strain abundance, less than 1.0 for strains growing more slowly than, and more than 1.0 for strains growing more quickly than the average growth rate of the pool.

Clustering to define four phenotypic classes was performed by the *k*-means method, employing the growth estimates (per strain per medium) with the GeneSpring statistical package (Silicon Genetics). We averaged the results of the two duplicate experiments for the homozygous diploid time course in relation to media YPD, YPDGE, YPG, YPE and YPL, and calculated the similarity between genes using standard correlation with a maximum of 100 iterations. Further clustering of genes within a group was carried out using hierarchical clustering.

Calculation of the enrichment factor was carried out using the formula $(a/b)/(c/d)$, where a is number of previously known mitochondrial proteins with a phenotype, b is the total number of genes with a phenotype, c is the number of previously known mitochondrial genes in the genome and d is the total number of genes in the genome. For expression analysis of the diauxic shift[19], we used the pool of genes that had at least either a doubling or a halving of expression ($a = 137$, $b = 1618$, $c = 425$, $d = 5965$, compared with $a = 201$ and $b = 466$ for our data, with spurious ORFs[12] removed from both data sets). Had we considered only genes with at least a doubling of expression, an enrichment factor of 2.2 would have been obtained.

Protein import into isolated mitochondria. For SP6 polymerase–driven synthesis of pre-proteins *in vitro*, we amplified the ORFs from ATG to STOP codon by PCR and cloned into the vector pGEM4 (Promega). Radiolabeled pre-proteins were synthesized by a coupled *in vitro* transcription–translation reaction in reticulocyte lysate (Promega) in the presence of [^{35}S]methionine. After isolating mitochondria from yeast strain W334 grown on lactate medium, we resuspended them at 25 °C in import buffer (0.3 mg/ml fatty acid–free BSA, 0.6 M sorbitol, 80 mM KCl, 10 mM magnesium acetate, 2 mM KH_2PO_4, 2.5 mM EDTA, 2.5 mM $MnCl_2$, 2 mM ATP, 5 mM NADH and 50 mM HEPES–KOH, pH 7.2). We initiated import by adding 1–10% (vol/vol) of reticulocyte lysate containing radiolabeled pre-protein. After 15 min, we placed the samples on ice for 15 min with or without proteinase K (50 μg/ml) to remove non-imported proteins. Protease was inhibited by the addition of 2 mM PMSF. We re-isolated mitochondria and analyzed them by SDS–PAGE and autoradiography. Control experiments were performed in the absence of membrane potential in the presence of 1 μM valinomycin and 20 μM oligomycin.

Human candidate disease gene analysis. We searched yeast ORFs using NCBI tBLASTN against UniGene using as the database Hs.seq.uniq[21] (Oct. 30, 2001 build), containing one sequence selected from each UniGene cluster. Searches were performed with an *E*-value cutoff of 10^{-4} and default values of all other parameters. Genes known to be mutated in human disease were also searched against the yeast genome; differences in the reciprocal BLAST searches were analyzed by hand. Genes known to be involved in human mitochondrial disease were considered only if genetic analysis had confirmed a gene mutation. Ortholog genome positions were identified and searched against diseases listed in the Online Mendelian Inheritance in Man (OMIM) database.

Online supplementary information. Fitness values and growth plots for each yeast deletion strain in each media condition are available online in a searchable database at http://www-deletion.stanford.edu/YDPM/YDPM_index.html. Other information was obtained from the yeast deletion project on http://yeastdeletion.stanford.edu/ and the MitoP database for mitochondrial-related genes, proteins and diseases at http://mips.gsf.de/proj/medgen/mitop/.

GenBank accession numbers. *ACAA2*, NM_006111; *ACO1*, NM_002197; *ALAS2*, NM_000032; *ALDH1B1*, NM_000692; *APEXL2*, BC007669; *ATP5A1*, NM_004046; *CGI-11*, NM_015941; *DKFZP667C165*, XM_042282; *DNAJA1*, NM_001539; *LOC85479*, NM_033105; *MGC14797*, NM_032335; *MGC14836*, NM_033412; *MRPL15*, NM_014175; *NDUFA1*, NM_004541; *NDUFB6*, NM_002493; *PDCD8*, NM_004208; *PDE7A*, XM_037534; *PFKFB1*, NM_002625; *PLS3*, NM_005032; *SLC9A6*, NM_006359; *SLC25A5*, NM_001152; *SLC25A14*, NM_003951; *SR-BP1*, NM_005866; *TIMM17B*, NM_005834.

Note: Supplementary information is available on the Nature Genetics website.

Acknowledgments

We thank M. Mindrinos, E. Allen, T. Neklesa, Q. Wang, W. Neupert and T. Meitinger for helpful advice and M. Trebo for help with preparing the supplementary website. This work was supported by the US National Institutes of Health (P.J.O. and R.W.D.) and the Bundesministerium für Bildung und Forschung (H.P.). L.M.S. was supported as a Howard Hughes Medical Institute predoctoral fellow and C.S. as a Deutsche Forschungsgemeinschaft postdoctoral fellow.

Competing interests statement

The authors declare that they have no competing financial interests.

Received 20 February; accepted 16 May 2002.

1. Foury, F. Human genetic diseases: a cross-talk between man and yeast. *Gene* **195**, 1–10 (1997).
2. DiMauro, S. & Schon, E.A. Nuclear power and mitochondrial disease. *Nature Genet.* **19**, 214–215 (1998).
3. Wallace, D.C. Mitochondrial diseases in man and mouse. *Science* **283**, 1482–1488 (1999).
4. Winzeler, E.A. *et al*. Functional characterization of the *S. cerevisiae* genome by gene deletion and parallel analysis. *Science* **285**, 901–906 (1999).
5. Birrell, G.W., Giaever, G., Chu, A.M., Davis, R.W. & Brown, J.M. A genome-wide screen in *Saccharomyces cerevisiae* for genes affecting UV radiation sensitivity. *Proc. Natl Acad. Sci. USA* **98**, 12608–12613 (2001).
6. Ooi, S.L., Shoemaker, D.D. & Boeke, J.D. A DNA microarray-based genetic screen for nonhomologous end-joining mutants in *Saccharomyces cerevisiae*. *Science* **294**, 2552–2556 (2001).
7. Shoemaker, D.D., Lashkari, D.A., Morris, D., Mittmann, M. & Davis, R.W. Quantitative phenotypic analysis of yeast deletion mutants using a highly parallel molecular bar-coding strategy. *Nature Genet.* **14**, 450–456 (1996).
8. Tzagoloff, A. & Myers, A.M. Genetics of mitochondrial biogenesis. *Annu. Rev. Biochem.* **55**, 249–285 (1986).
9. Yaffe, M.P. in *Methods in Enzymology* Vol. 194 (eds Guthrie, C. & Fink, G.R.) 627–643 (Academic Press, San Diego, California, 1991).
10. Scharfe, C. *et al*. MITOP, the mitochondrial proteome database: 2000 update. *Nucleic Acids Res.* **28**, 155–158 (2000).
11. Grivell, L.A. *et al*. Mitochondrial assembly in yeast. *FEBS Lett.* **452**, 57–60 (1999).
12. Wood, V., Rutherford, K.M., Ivens, A., Rajandream, M.A. & Barrell, B. A re-annotation of the *Saccharomyces cerevisiae* genome. *Comp. Funct. Genom.* **2**, 143–154 (2001).
13. Claros, M.G. & Vincens, P. Computational method to predict mitochondrially imported proteins and their targeting sequences. *Eur. J. Biochem.* **241**, 779–786 (1996).
14. Andersson, S.G. *et al*. The genome sequence of *Rickettsia prowazekii* and the origin of mitochondria. *Nature* **396**, 133–140 (1998).
15. Schwikowski, B., Uetz, P. & Fields, S. A network of protein–protein interactions in yeast. *Nature Biotechnol.* **18**, 1257–1261 (2000).
16. Kumar, A. *et al*. Subcellular localization of the yeast proteome. *Genes Dev.* **16**, 707–719 (2002).
17. Nishino, I., Spinazzola, A. & Hirano, M. Thymidine phosphorylase gene mutations in MNGIE, a human mitochondrial disorder. *Science* **283**, 689–692 (1999).
18. Ashe, M.P., De Long, S.K. & Sachs, A.B. Glucose depletion rapidly inhibits translation initiation in yeast. *Mol. Biol. Cell* **11**, 833–848 (2000).
19. DeRisi, J.L., Iyer, V.R. & Brown, P.O. Exploring the metabolic and genetic control of gene expression on a genomic scale. *Science* **278**, 680–686 (1997).
20. Hughes, T.R. *et al*. Functional discovery via a compendium of expression profiles. *Cell* **102**, 109–126 (2000).
21. Boguski, M.S. & Schuler, G.D. ESTablishing a human transcript map. *Nature Genet.* **10**, 369–371 (1995).
22. Mewes, H.W. *et al*. MIPS: a database for genomes and protein sequences. *Nucleic Acids Res.* **28**, 37–40 (2000).
23. Hentati, A. *et al*. Linkage of 'pure' autosomal recessive familial spastic paraplegia to chromosome 8 markers and evidence of genetic locus heterogeneity. *Hum. Mol. Genet.* **3**, 1263–1267 (1994).
24. Christodoulou, K. *et al*. Mapping of the second Friedreich's ataxia (FRDA2) locus to chromosome 9p23–p11: evidence for further locus heterogeneity. *Neurogenetics* **3**, 127–132 (2001).
25. Kerrison, J.B. *et al*. Genetic heterogeneity of dominant optic atrophy, Kjer type: identification of a second locus on chromosome 18q12.2–12.3. *Arch. Ophthalmol.* **117**, 805–810 (1999).
26. Assink, J.J. *et al*. A gene for X-linked optic atrophy is closely linked to the Xp11.4–Xp11.2 region of the X chromosome. *Am. J. Hum. Genet.* **61**, 934–939 (1997).
27. Priest, J.M., Fischbeck, K.H., Nouri, N. & Keats, B.J. A locus for axonal motor-sensory neuropathy with deafness and mental retardation maps to Xq24–q26. *Genomics* **29**, 409–412 (1995).
28. McMullan, T.F., Collins, A.R., Tyers, A.G. & Robinson, D.O. A novel X-linked dominant condition: X-linked congenital isolated ptosis. *Am. J. Hum. Genet.* **66**, 1455–1460 (2000).
29. Malmgren, H. *et al*. Linkage mapping of a severe X-linked mental retardation syndrome. *Am. J. Hum. Genet.* **52**, 1046–1052 (1993).